Journal of Power Sources 187 (2009) 387–392

Contents lists available at ScienceDirect

Journal of Power Sources

journal homepage: www.elsevier.com/locate/jpowsour

Performance of alkaline electrolyte-membrane-based direct ethanol fuel cells

Y.S. Li, T.S. Zhao*, Z.X. Liang

Department of Mechanical Engineering, The Hong Kong University of Science and Technology, Clear Water Bay, Kowloon, Hong Kong SAR, China

ARTICLE INFO

Article history:
Received 4 July 2008
Received in revised form 4 September 2008
Accepted 20 October 2008
Available online 18 November 2008

Keywords:
Anion-exchange membrane
Direct ethanol fuel cell
Hydroxyl ions
Non-platinum catalyst
Cell performance
Power density

ABSTRACT

A single alkaline direct ethanol fuel cell (alkaline DEFC) with an anion-exchange membrane and non-platinum (non-Pt) catalysts is designed, fabricated, and tested. Particular attention is paid to investigating the effects of different operating parameters, including the cell operating temperature, concentrations of both ethanol and the added electrolyte (KOH) solution, as well as the mass flow rates of the reactants. The alkaline DEFC yields a maximum power density of 60 mW cm^{-2}, a limiting current density of about 550 mA cm^{-2}, and an open-circuit voltage of about 900 mV at 40 °C. The experimental results show that the cell performance is improved on increasing the operating temperature, but there exists an optimum ethanol concentration under which the fuel cell has the best performance. In addition, cell performance increases monotonically with increasing KOH concentration in the region of low current density, while in the region of high current density, there exists an optimum KOH concentration in terms of cell performance. The effect of flow rate of the fuel solution is negligible when the ethanol concentration is higher than 1.0 M, although the cell performance improves on increasing the oxygen flow rate.

1. Introduction

Direct alcohol fuel cells (DAFCs) are electrochemical devices that directly convert the chemical energy stored in liquid alcohol (e.g., methanol and ethanol) into electricity. DAFCs have many advantages compared with hydrogen-feed fuel cells, including higher energy densities, facile liquid storage, and simpler system structures [1–9]. These benefits suggest that this type of fuel cell is a promising power source for portable and other mobile applications. Over the past decade, special attention has been paid to fuel cells that use methanol as the fuel, namely direct methanol fuel cells (DMFCs), mainly because methanol is the simplest alcohol and potentially has better electrode kinetics than other alcohol fuels. However, in addition to other technical problems encountered in the development of this type of fuel cell, the toxicity of methanol is another issue that limits the wide application of DMFCs. By comparison, ethanol is more environmentally friendly and can be easily produced in large quantities from agricultural products or biomass. Hence, direct ethanol fuel cells (DEFCs) have recently received increased attention.

Based on the electrolyte membrane used, DEFCs can be divided into two types: acid- and alkaline-membrane DEFCs. A considerable amount of effort has been devoted to acid DEFCs; as a result, significant progress has been made in their development [1–3]. For example, Xin and co-workers [1,2] developed a highly active PtSn catalyst for the ethanol oxidation reaction (EOR) in an acid medium; the application of this electrocatalyst to the anode of the DEFC resulted in a maximum power density of 60 mW cm^{-2} at 90 °C, the highest performance reported in the open literature [1]. Although the performance seems appealing, the commercialization of acid DEFCs has been hindered by several issues. First, the slow kinetics of the EOR in acid media leads to a serious activation polarization loss, thereby diminishing cell performance. Second, the electrocatalyst (e.g., PtSn) suffers from corrosion in acid DEFCs, which results in poor durability of the fuel cell. Another critical obstacle that limits the wide application of acid DEFCs is the cost: acid electrolyte membranes (typically Nafion® material) are expensive; and a considerable amount of precious Pt is needed to achieve decent performance in acid DEFCs. All these issues can be alleviated when acid membranes are replaced by alkaline membranes. The most striking feature of alkaline DEFCs is their quicker kinetics of the oxygen reduction reaction (ORR) in alkaline media, even with low-cost non-platinum metals as the electrocatalyst. Another important feature of alkaline DEFCs is the use of a non-Pt electrocatalyst on the cathode eliminates the oxidation of the fuel that may be transported from the anode, which makes the cathode potential much higher than in acid DEFCs. Because of these important features, alkaline DEFCs have recently attracted increasing attention [4–9]. So far, effort has mainly been concentrated on the synthesis of alkaline membranes and electrocatalysts for the EOR and ORR in alkaline media [10–19]. Stoica and co-worker [15] prepared an alkaline membrane that was composed of two cyclic diamines and

* Corresponding author. Tel.: +852 2358 8647.
E-mail address: metzhao@ust.hk (T.S. Zhao).

0378-7753/$ – see front matter © 2008 Elsevier B.V. All rights reserved.
doi:10.1016/j.jpowsour.2008.10.132

demonstrated that this membrane was good in terms of ionic conductivity and thermal stability up to 220 °C. Recently, Slade and co-worker [16] prepared a series of FEP-based alkaline membranes via a radiation-grafting method and showed that the OH^- conductivity could be as high as 0.023 S cm^{-1} at 50 °C. On the development of electrocatalysts for the ORR and EOR, Ogumi and co-workers [17] prepared a carbon-supported $La_{1-x}Sr_xMnO_3$ (LSM/C) cathode catalyst and studied its catalytic activities for the ORR under the existence of ethylene glycol (EG) by using a rotating disk electrode. The experiment results indicated that LSM/C can serve as a cathode catalyst in alkaline direct EG fuel cells with no mixed potential problem. Shen and co-worker [18] investigated the addition of tungsten carbide nanocrystals to the Ag based electrocatalysts for the ORR and demonstrated that the composite catalyst yielded a unique selectivity for the ORR in alcohol-containing solutions and was immune to methanol, ethanol, isopropanol and glycerol. More recently, Shen and co-worker [19] synthesized a hexagonal tungsten carbide single nanocrystal-supported Pd electrocatalyst and demonstrated that this catalyst had extremely high electrocatalytic activity for the EOR as a result of the synergistic interaction between Pd and WC.

Our literature review indicates that past efforts in developing alkaline DEFCs have been devoted mainly to the development of alkaline membranes and electrocatalysts, whereas system design and development of DEFCs have not yet been addressed. The objective of this work is to develop a single alkaline DEFC with commercial alkaline membranes from Tokuyama and HYPERMEC™ catalysts from Acta. Particular attention is paid to a systematic investigation of the effects of various operating parameters on cell performance, namely, cell operating temperature, concentrations of ethanol and KOH solutions, and flow rates of reactants.

2. Experimental

2.1. Membrane electrode assembly

The membrane electrode assembly (MEA), with an active area of 2.0 cm × 2.0 cm, consisted of two single-sided electrodes and an anion-exchange membrane. Both the anode and cathode electrodes with non-platinum HYPERMEC™ catalysts were provided by Acta. The catalyst loadings in the anode and cathode were 2.0 and 1.0 mg cm^{-2}, respectively. While the membrane (A201), with a thickness of 28 μm, was provided by Tokuyama. The anode and cathode backing layers were made of nickel foam (Hohsen Corp., Japan) and carbon cloth (ETEK), respectively. Finally, the MEA was formed by sandwiching the membrane between the two electrodes that were attached with cell fixtures, as described below.

2.2. Single-cell fixture

The single-cell fixture consisted of two current-collector plates that were made of 316L stainless steel. On one side of each current-collector plate, a single serpentine flow field was grooved by the wire-cut technique. The channel was 1.0 mm wide and 0.5 mm deep; the channel rib width was 1.0 mm.

2.3. Cell test station and test conditions

In this work, an Arbin BT2000 (Arbin Instrument Inc.) combined with a computer interface and a system of electrical load controllers, was employed to measure the voltage–current (polarization) curves. The cell resistance was measured by the dc-pulse method. An aqueous fuel solution containing ethanol and potassium hydroxide (KOH) was pumped to the anode by a peristaltic pump. Simultaneously, 99.7% pure oxygen was fed to the cathode without humidification; the flow rate of the oxygen was controlled and measured by a mass flow controller (Omega FMA-7105E). In addition, the cell operating temperature was measured with a thermocouple located at the anode current-collector; two electrical heating rods were installed in the fixture to control the operating temperature during the experiments.

3. Results and discussion

3.1. General performance

Fig. 1 shows the polarization and power-density curves of the alkaline DEFC with non-Pt catalysts both at the anode and cathode, and an anion-exchange membrane. The experiment was performed at 40 °C with an aqueous solution of 3.0 M ethanol mixed with 7.0 M KOH pumped to the anode at a rate of 2.0 ml min^{-1} and with dry pure oxygen at a flow rate of 100 standard cubic centimeters per minute (sccm) fed to the cathode. A maximum power density of 60 mW cm^{-2} is achieved at a current density of 250 mA cm^{-2}, which is much higher than that of the alkaline DMFCs using Pt catalysts as reported elsewhere [20]. More significantly, the open-circuit voltage (OCV) of the present alkaline DEFC is as high as 900 mV, i.e., 100 mV higher than that of an alkaline direct ethylene-glycol fuel cell [4], and about 200 mV higher than that of a conventional acid DMFC with a Nafion membrane [21]. The substantially better performance achieved with the alkaline DEFC can be explained by the superior electrocatalytic activity of the HYPERMEC™ catalysts for the EOR and the ORR in alkaline media.

3.2. Effect of cell operating temperature

Cell polarization and power density curves at different operating temperatures from 30 to 60 °C are presented in Fig. 2. The cell performance improves as the temperature is increased over the whole current density region, including the activation, ohmic and concentration-controlled regions. The maximum power density is 12 mW cm^{-2} at 30 °C and it almost triples to 30 mW cm^{-2} at 60 °C. The reasons why the performance improves as the operating temperature increases are as follows. First, an increase in the temperature accelerates the electrochemical kinetics of both

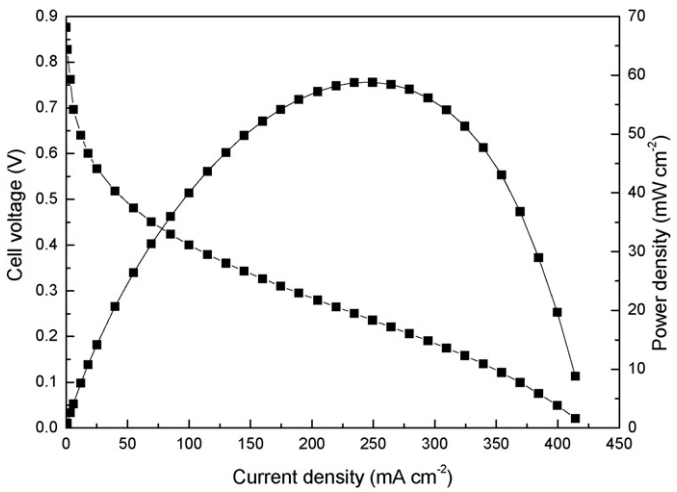

Fig. 1. Polarization curves and power density curves of alkaline DEFCs. Anode: 3.0 M ethanol and 7.0 M KOH aqueous solution, 2.0 ml min^{-1}. Cathode: pure oxygen, 100 sccm. Temperature: 40 °C.

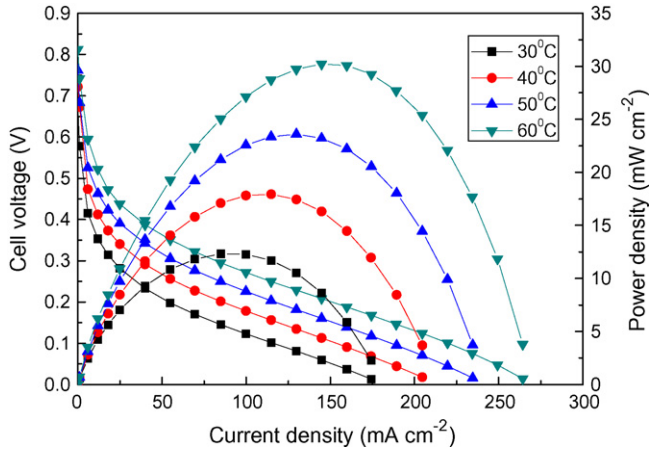

Fig. 2. Effect of temperature on cell polarization and power density. Anode: 1.0 M ethanol and 1.0 M KOH aqueous solution, 1.0 ml min^{-1}. Cathode: pure oxygen, 100 sccm.

the EOR at the anode and the ORR at the cathode, which consequently increases the cell voltage. This can be further confirmed by the OCV data shown in Fig. 3. The OCV increases from 0.67 to 0.82 V as the temperature is increased from 30 to 60 °C. Second, the conductivity of the OH^- ion increases with increasing temperature, and this leads to a smaller ohmic loss, as evidenced by the cell resistance shown in Fig. 3. The cell resistance decreases as the cell temperature is increased. As a result, cell performance is improved. Furthermore, both the ethanol and oxygen transport diffusivities increase with increasing temperature. As a result, the improved transfer of the ethanol and oxygen results in higher reactant concentrations at both the anode and cathode catalyst layers such that the polarization losses due to mass transfer are lowered. In summary, improvement in the performance of the fuel cells with increasing operating temperature is due to the faster electrochemical kinetics, increased conductivity of the OH^- ions, and enhanced mass transfer. The results presented in Fig. 2 demonstrate that the temperature is a key parameter affecting cell performance.

3.3. Effect of ethanol concentration

The effect of ethanol concentration on cell performance when the alkaline concentration is fixed at 1.0 M KOH is shown in Fig. 4.

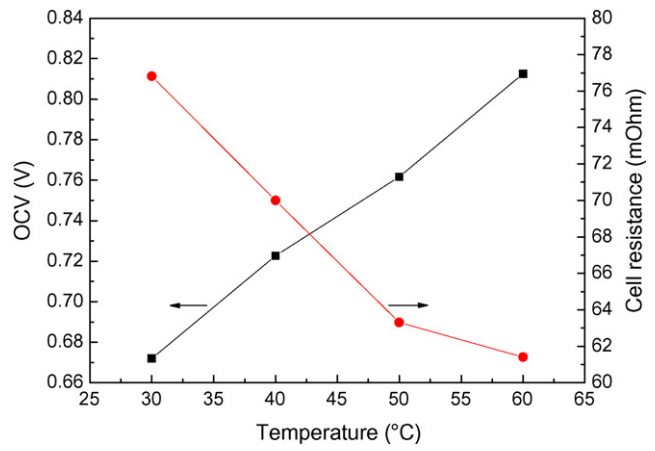

Fig. 3. Effect of temperature on open-circuit voltage and cell resistance. Anode: 1.0 M ethanol and 1.0 M KOH aqueous solution, 1.0 ml min^{-1}. Cathode: pure oxygen, 100 sccm.

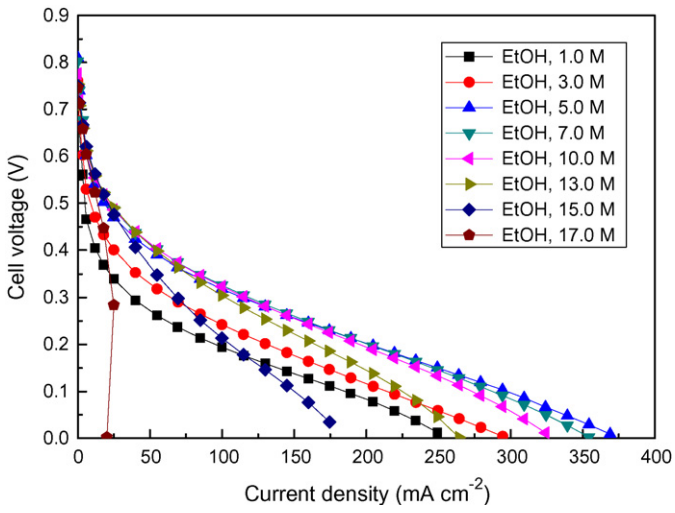

Fig. 4. Effect of ethanol concentration on cell polarization. Anode: 1.0 M KOH containing various ethanol concentration aqueous solutions, 2.0 ml min^{-1}. Cathode: pure oxygen, 100 sccm. Temperature: 40 °C.

In the low current density region (lower than 50 mA cm^{-2}), the voltage increases as the ethanol concentration is raised from 1.0 to 13.0 M. For a given electrocatalyst, the EOR kinetics depend mainly on the local concentrations of both ethanol and OH^- ions. The reason for the higher voltages with higher ethanol concentrations in the low current density region is because the local ethanol concentration in the catalyst layer increases from a starving to a sufficient amount when the ethanol concentration is increased from 1.0 to 13.0 M. However, a further increase in the ethanol concentration, for instance, to 15.0 or 17.0 M, causes the voltage to decrease gradually in the low current density region. This is because the high ethanol concentration causes more active sites to be covered by ethanol, which may block the adsorption of hydroxyl on the active sites [22]. Hence, the cell performance declines when the ethanol concentration is higher than 13.0 M.

At high current densities, the alkaline DEFC yields the best performance with an ethanol concentration of 5.0 M; either a higher or lower ethanol concentration results in worse performance. Very concentrated ethanol may create a barrier for the transfer of hydroxyl ions, giving rise to an increase in cell resistance and a lowering of cell performance [23,24]. An increase in cell resistance with increasing ethanol concentration is evident in Fig. 5. The cell

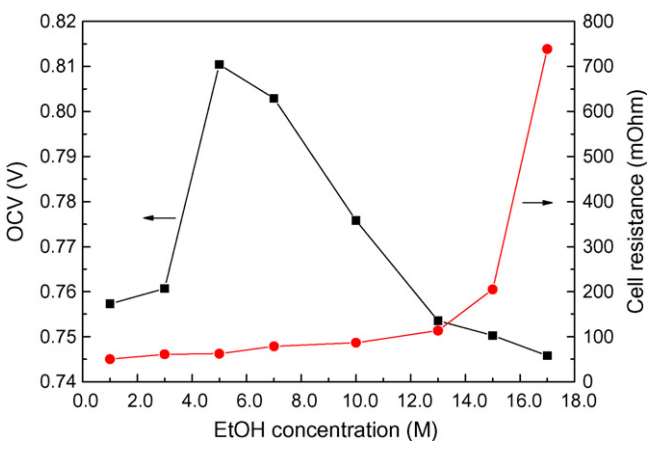

Fig. 5. Effect of ethanol concentration on open-circuit voltage and cell resistance. Anode: 1.0 M KOH containing various ethanol concentration aqueous solutions, 2.0 ml min^{-1}. Cathode: pure oxygen, 100 sccm. Temperature: 40 °C.

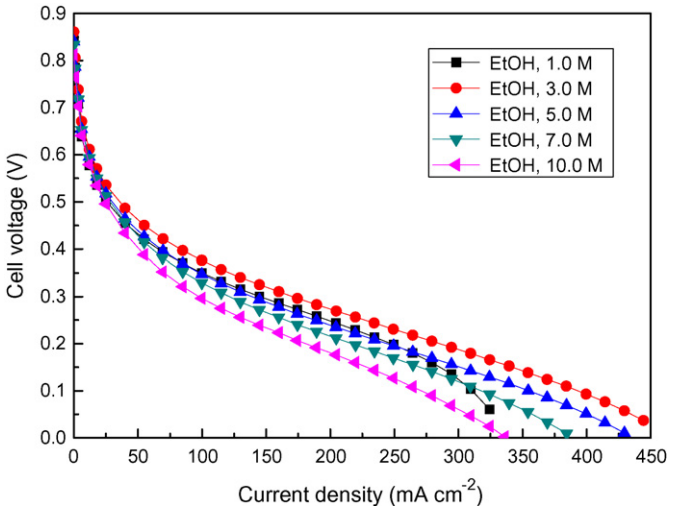

Fig. 6. Effect of ethanol concentration on cell polarization. Anode: 5.0 M KOH containing various ethanol concentration aqueous solutions, 2.0 ml min^{-1}. Cathode: pure oxygen, 100 sccm. Temperature: 40 °C.

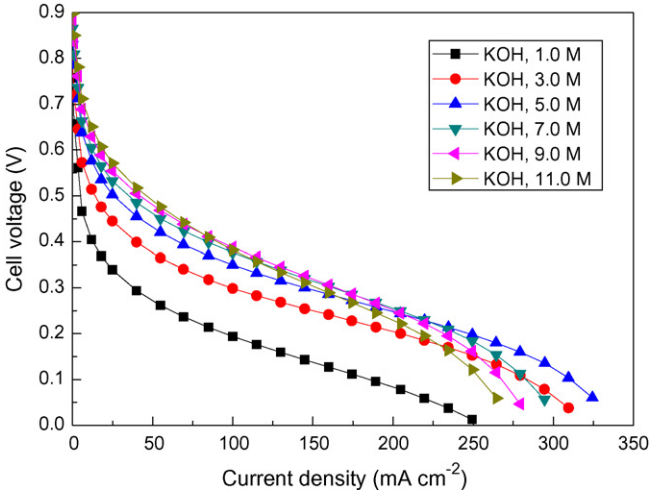

Fig. 8. Effect of KOH concentration on cell polarization. Anode: 1.0 M ethanol containing various KOH concentration aqueous solutions, 2.0 ml min^{-1}. Cathode: pure oxygen, 100 sccm. Temperature: 40 °C.

resistance becomes extremely high when the ethanol concentration is raised to 17.0 M. This is why Fig. 4 shows a rapid drop in voltage with 17.0 M ethanol concentration.

Fig. 5 also shows the variation in the OCV with the ethanol concentration. The OCV first increases, reaches a maximum at about 5.0 M, and then decreases with increasing ethanol concentration. The reason why the OCV increases with ethanol concentration is because the local ethanol concentration in the catalyst layer is too low when ethanol solution below 5.0 M is fed to the cell and results in poor anode performance. However, when the ethanol concentration is sufficiently high at the anode, the coverage of hydroxide ions on catalytic sites may be reduced, resulting in an increase in the anode overpotential. Therefore, the variation in the OCV with ethanol concentration shown in Fig. 5 is the result of the competition between the ethanol coverage and the hydroxide ion coverage towards the kinetics of the EOR.

Experiments were also performed when the KOH concentration was increased to 5.0 M while keeping all other conditions the same as those in Fig. 4. The measured polarization curves are shown in Fig. 6, while the variations in OCV and cell resistance with ethanol concentration are presented in Fig. 7. The data in Fig. 6 show a similar trend to those in Fig. 4 for the weaker KOH concentration. Correspondingly, similar trends in the variation of OCV and cell resistance to those shown in Fig. 5 can also be observed in Fig. 7 for the stronger KOH concentration. In summary, for a given KOH concentration, there exists an optimum ethanol concentration at which the fuel cell yields its best performance.

3.4. Effects of KOH concentrations

The alkalinity of the anode environment significantly affects not only the electrochemical kinetics but also the transfer of species to the anode [22,25]. To study the influence of the electrolyte on cell performance, 1.0 and 5.0 M ethanol aqueous solutions with various KOH concentrations were tested.

Polarization curves for different KOH concentrations ranging from 1.0 to 11.0 M at a fixed ethanol concentration of 1.0 M are presented in Fig. 8. The voltage increases with increasing KOH concentration in the low current density region (lower than 150 mA cm^{-2}). This is because a higher KOH concentration can provide more OH^- ions in the anode catalyst layer, leading to faster EOR kinetics so that the anode overpotential decreases with increasing

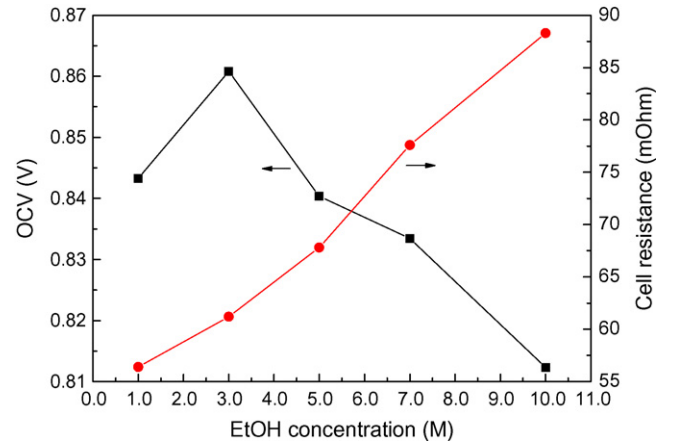

Fig. 7. Effect of ethanol concentration on open-circuit voltage and cell resistance. Anode: 5.0 M KOH containing various ethanol concentration aqueous solutions, 2.0 ml min^{-1}. Cathode: pure oxygen, 100 sccm. Temperature: 40 °C.

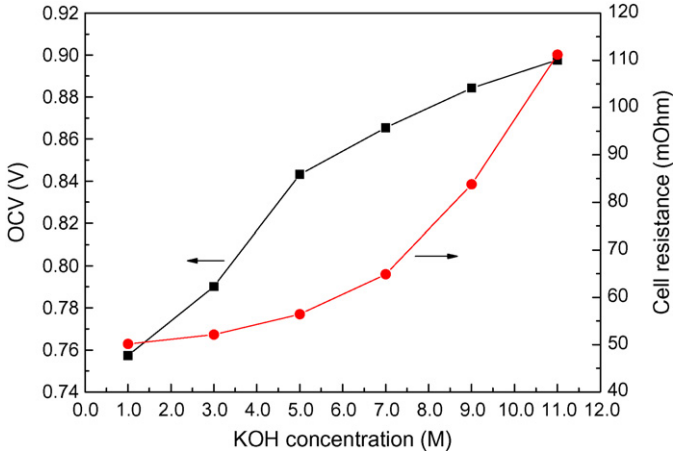

Fig. 9. Effect of KOH concentration on open-circuit voltage and cell resistance. Anode: 1.0 M ethanol containing various KOH concentration aqueous solutions, 2.0 ml min^{-1}. Cathode: pure oxygen, 100 sccm. Temperature: 40 °C.

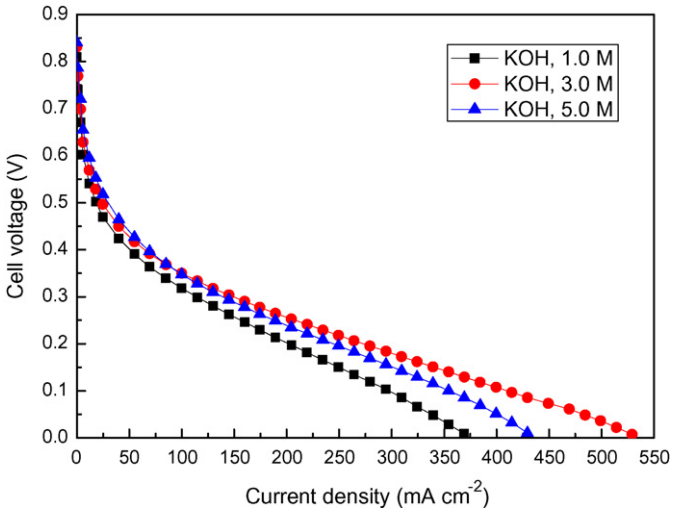

Fig. 10. Effect of KOH concentration on cell polarization. Anode: 5.0 M ethanol containing various KOH concentration aqueous solutions, 2.0 ml min^{-1}. Cathode: pure oxygen, 100 sccm. Temperature: 40 °C.

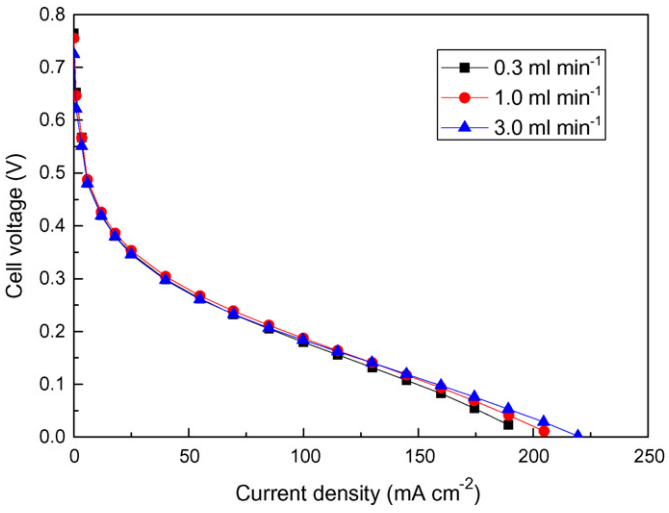

Fig. 12. Cell polarization with different anode flow rates. Anode: 1.0 M ethanol and 1.0 M KOH aqueous solution, 0.3–3.0 ml min^{-1}. Cathode: pure oxygen, 100 sccm. Temperature: 40 °C.

KOH concentration. This suggests that in the low current density region, the concentration of OH^- ion is the predominant factor that determines the anode potential. This point is further confirmed by the OCV behaviour shown in Fig. 9 that is, the OCV increases with increasing KOH concentration. It must be pointed out that the increase in KOH concentration is limited by its solubility in ethanol solutions. With the present ethanol concentration, the KOH concentration cannot be higher than 13.0 M.

Unlike the situation in the low current density region, the voltage falls in the high current density region when the KOH concentration is increased above 5.0 M. The explanation for this is found in the data of Fig. 9. The increase in the cell resistance with increasing KOH concentration is caused by the increased anode OH^- concentration, which resists the transport of OH^- ions from the cathode to the anode.

Experiments were also conducted by increasing the ethanol concentration to 5.0 M while keeping all the other conditions the same as those in Fig. 8. The resulting polarization curves are given in Fig. 10, while the variations in OCV and cell resistance with KOH concentration are presented in Fig. 11. The data in Fig. 10 show a similar trend to those in Fig. 8. Correspondingly, Fig. 9 shows a similar trend to Fig. 11. In summary, the cell voltage in the current density region increases with increased KOH concentration. The maximum KOH concentration is limited, however, by its solubility in ethanol solutions. On the other hand, in the high current density region, there exists an optimum KOH concentration with which the fuel cell can yield the best performance.

3.5. Effects of mass flow rates of fuel solutions and oxygen

Fig. 12 shows the effect of different fuel solution flow rates on cell performance from 0.3 to 3.0 ml min^{-1} at 40 °C, while keeping the oxygen flow rate at 100 sccm. The effect of the fuel solution flow rate is rather small in the low current density region, but the cell performance improves slightly with increasing solution flow rate in the high current density region. This latter feature is attributed to the enhanced mass-transfer of both ethanol and OH^- ions from the flow-field to the catalyst layer. In general, the experimental data presented in Fig. 12 suggest that the effect of fuel flow rate on cell performance is insignificant when the ethanol concentration is greater than 1.0 M.

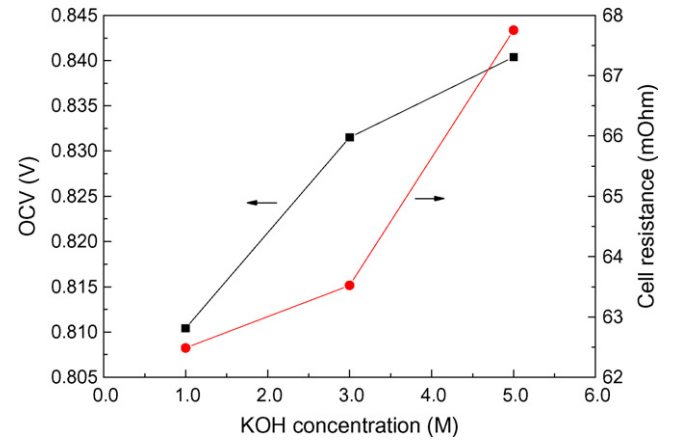

Fig. 11. Effect of KOH concentration on open-circuit voltage and cell resistance. Anode: 5.0 M ethanol containing various KOH concentration aqueous solutions, 2.0 ml min^{-1}. Cathode: pure oxygen, 100 sccm. Temperature: 40 °C.

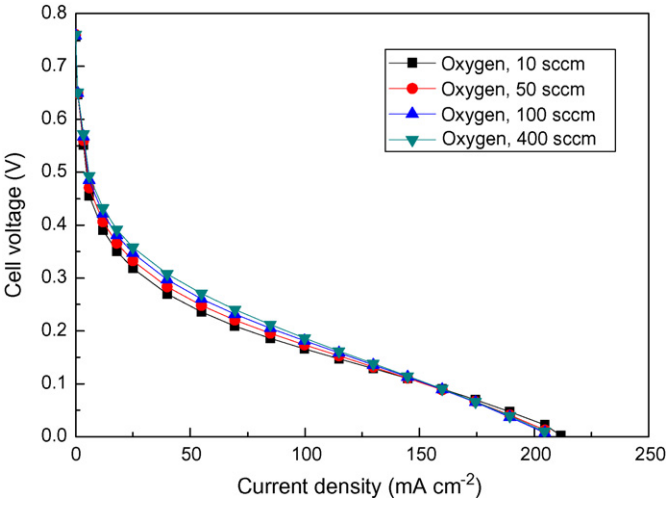

Fig. 13. Cell polarization with different oxygen flow rates. Anode: 1.0 M ethanol and 1.0 M KOH aqueous solution, 1.0 ml min^{-1}. Cathode: pure oxygen, 10–400 sccm. Temperature: 40 °C.

The effect of oxygen flow rate on cell performance is illustrated in Fig. 13. The experiments were performed with the fuel solution (1.0 M ethanol and 1.0 M KOH) fed at a rate of 1.0 ml min^{-1}. Although not substantial, the cell voltage increases as the oxygen flow rate increased. The improved performance can be attributed to the enhanced ORR as a result of the enhanced mass transport of oxygen at higher flow rates.

4. Conclusions

A single alkaline DEFC with an anion-exchange membrane and non-Pt catalysts has been developed and tested under different operating conditions. The experimental results show that the alkaline DEFC can yield a maximum power density of 60 mW cm^{-2} at 40 °C, a maximum current density of about 550 mA cm^{-2}, and an open-circuit voltage of about 900 mV. These results suggest that the alkaline DEFC is superior to all other similar DAFCs in terms of performance. The cell performance improves with increasing cell temperature due to the improved kinetics of the EOR and ORR and increases in ethanol diffusivity and hydroxyl ion conductivity. Tests with different ethanol concentrations show that for a given KOH concentration, there is an optimum ethanol concentration at which the fuel cell can yield its best performance. With respect to the effect of the KOH concentration, in the low current density region, the cell voltage increases with increasing KOH concentration. In the high current density region, however, there is an optimum KOH concentration that yields the best cell performance. Tests with different reactant flow rates indicate that the effect of flow rate of the fuel solution on cell performance is insignificant when the ethanol concentration is above than 1.0 M, although an increase in oxygen flow rate can yield superior cell performance.

Acknowledgements

The work was fully supported by a grant from the Research Grants Council of the Hong Kong Special Administrative Region, China (Project No. 622807) and by the Joint Research Fund for Hong Kong and Macao Young Scholars (Project No. 50629601). The material support from Acta and Tokuyama is greatly acknowledged.

References

[1] W.J. Zhou, S.Q. Song, W.Z. Li, Z.H. Zhou, G.Q. Sun, Q. Xin, S. Douvartzides, P. Tsiakaras, J. Power Sources 140 (2005) 50–58.
[2] S.Q. Song, W.J. Zhou, Z.X. Liang, R. Cai, G.Q. Sun, Q. Xin, V. Stergiopoulos, P. Tsiakaras, Appl. Catal. B: Environ. 55 (2005) 65–72.
[3] C. Coutanceau, L. Demarconnay, C. Lamy, J.M. Leger, J. Power Sources 156 (2006) 14–19.
[4] K. Matsuoka, Y. Iriyama, T. Abe, M. Matsuoka, Z. Ogumi, J. Power Sources 150 (2005) 27–31.
[5] P.K. Shen, C.W. Xu, R. Zeng, Y.L. Liu, Electrochem. Solid State Lett. 9 (2006) A39–A42.
[6] J. Bagchi, S.K. Bhattacharya, J. Power Sources 163 (2007) 661–670.
[7] P. Paul, J. Bagchi, S.K. Hattacharya, Indian J. Chem.: Sect. A 45 (2006) 1144–1152.
[8] V. Rao, C. Hariyanto, U. Cremers, Stimming, Fuel Cells 7 (2007) 417–423.
[9] Z. Ogumi, K. Matsuoka, S. Chiba, M. Matsuoka, Y. Iriyama, T. Abe, M. Inaba, Electrochemistry 70 (2002) 980–983.
[10] J.S. Spendelow, A. Wieckowski, Phys. Chem. Chem. Phys. 9 (2007) 2654–2675.
[11] E. Gülzow, M. Schulze, J. Power Sources 127 (2004) 243–251.
[12] K. Matsuoka, M. Inaba, Y. Iriyama, T. Abe, Z. Ogumi, M. Matsuoka, Fuel Cells 2 (2002) 35–39.
[13] J.R. Varcoe, R.C.T. Slade, Fuel Cells 5 (2005) 187–200.
[14] M.R. Tarasevich, Z.R. Karichev, V.A. Bogdanovskaya, E.N. Lubnin, A.V. Kapustin, Electrochem. Commun. 7 (2005) 141–146.
[15] D. Stoica, L. Ogier, L. Akrour, F. Alloin, J.F. Fauvarque, Electrochim. Acta 53 (2007) 1596–1603.
[16] R.C.T. Slade, J.R. Varcoe, Solid State Ionics 176 (2005) 585–597.
[17] K. Miyazaki, N. Sugimura, K. Matsuoka, Y. Iriyama, T. Abe, M. Matsuoka, Z. Ogumi, J. Power Sources 178 (2008) 683–686.
[18] H. Meng, P.K. Shen, Electrochem. Commun. 8 (2006) 588–594.
[19] F.P. Hu, P.K. Shen, J. Power Sources 173 (2007) 877–881.
[20] E.H. Yu, K. Scott, J. Appl. Electrochem. 35 (2005) 91–96.
[21] H. Yang, T.S. Zhao, Q. Ye, J. Power Sources 139 (2005) 79–90.
[22] K. Scott, E. Yu, G. Vlachogiannopoulos, M. Shivare, N. Duteanu, J. Power Sources 175 (2008) 452–457.
[23] A. Verma, S. Basu, J. Power Sources 168 (2007) 200–210.
[24] E.H. Yu, K. Scott, J. Power Sources 137 (2004) 248–256.
[25] J.S. Park, S.H. Park, S.D. Yim, Y.G. Yoon, W.Y. Lee, C.S. Kim, J. Power Sources 178 (2008) 620–626.